

# Integrated exposomics/metabolomics for rapid exposure and effect analyses

Mira Flasch<sup>1,2</sup>, Veronika Fitz<sup>2,3</sup>, Evelyn Rampler<sup>3</sup>, Chibundu N. Ezekiel<sup>4</sup>, Gunda Koellensperger<sup>3,5</sup>, Benedikt Warth<sup>1,5\*</sup>

<sup>1</sup>University of Vienna, Faculty of Chemistry, Department of Food Chemistry and Toxicology, Währinger Straße 38-40, 1090 Vienna, Austria

<sup>2</sup>University of Vienna, Vienna Doctoral School of Chemistry, Währinger Straße 42, 1090, Vienna, Austria

<sup>3</sup>University of Vienna, Faculty of Chemistry, Department of Analytical Chemistry, Währinger Straße 38-40, 1090 Vienna, Austria

<sup>4</sup>Department of Microbiology, Babcock University, Ilishan Remo, Ogun State, Nigeria

<sup>5</sup>Exposome Austria, Research Infrastructure and National EIRENE Hub, Austria

**ABSTRACT:** Environmental drivers of disease susceptibility, referred to as the exposome in its totality, are poorly understood. Measuring the myriad of chemicals that humans are exposed to is immensely challenging and identifying disrupted metabolic pathways is an even more complex task. Here, we present a novel technological approach for the comprehensive, rapid and integrated analysis of the endogenous human metabolome and the chemical exposome. By combining reverse-phase and hydrophilic interaction liquid chromatography and fast polarity switching, molecules with highly diverse chemical structures can be analyzed in 15 minutes with a single analytical run. Standard reference materials and authentic standards were evaluated to critically benchmark performance. Highly sensitive median limits of detection with 0.04  $\mu\text{M}$  for >140 quantitatively assessed endogenous metabolites and 0.08 ng/mL for the >100 model xenobiotics were obtained. To prove the dual-column approach's applicability, real-life samples from sub-Saharan Africa (high exposure scenario) and Europe (low exposure scenario) were assessed in a targeted and non-targeted manner. Our LC-HRMS approach demonstrates the feasibility to quantitatively and simultaneously assess the endogenous metabolome and the chemical exposome for the high-throughput measurement of environmental drivers of disease.

## INTRODUCTION

Since the 'exposome' first emerged as a new paradigm in environmental health describing the entity of all environmental exposures enclosing lifestyle factors throughout a human's lifespan (Wild 2005), its scope has further been expanded. In recent definitions, endogenous metabolites involved in biological responses (i.e. the endogenous metabolome) that have been triggered by external exposures are typically included (Miller et al. 2014; Rappaport et al. 2014).

Comprehensive liquid chromatography high resolution mass spectrometry (LC-HRMS)-based approaches hold the promise to more comprehensively elucidate the exposome in future exposome-wide association studies (ExWAS). A broad spectrum of small molecules with diverse chemical properties ranging from endogenous metabolites to environmental xenobiotics can be determined with this technique. External stressors including xenobiotics and environmental changes are measured at the same

time as phenotypical changes in response to these exposures. Thus, LC-HRMS is an ideal platform for developing more holistic methods to study the exposome (Vermeulen et al. 2020). Its applicability to investigate the impact of environmental toxicants on the endogenous metabolome has previously been showcased (Warth et al. 2017; Johnson et al. 2012). Metabolomics has been applied in large metabolome-wide association studies (MWAS) to investigate biological mechanisms of diseases, their diagnosis and treatment. Several studies succeeded in deriving biological effects from their data, although data interpretation remains a challenge (Garratt et al. 2018; Reinke et al. 2017; Ganna et al. 2014; Rhoades et al. 2017; Hu et al. 2021). The approach plays also an important role in biomarker discovery and personalized medicine (Jacob et al. 2019). However, the study of external stressors and complex environmental exposures is clearly less explored and constitutes the next frontier in the current era of omic-scale exposure measurement and systems toxicology.

Targeted multi-analyte methods are commonly used for human biomonitoring (HBM) of xenobiotics, although most approaches assess only a relatively limited number of different exposure markers or chemical classes (Prasain et al. 2010; Vela-Soria et al. 2011; Azzouz et al. 2016; de Oliveira et al. 2019; Kolatorova Sosvorova et al. 2017; Braun et al. 2018; Šarkanj et al. 2018). However, recent initiatives aim to expand the coverage of such multi-analyte and multi-class HBM methods to a larger range of xenobiotics as exemplified e.g. Jamnik et al. (2022) who simultaneously assessed more than eighty chemicals with known affinity to the estrogen receptor in relevant biological specimen (blood, urine and breast milk).

The vast physico-chemical diversity of xenobiotics implies also a widely varying toxicological effects of them on humans. The adverse impact of e.g. mycotoxins, a group of fungal food toxins, range from liver carcinogenicity (aflatoxins), nephrotoxicity (ochratoxin A), estrogenicity (zearalenone) to inhibition of protein synthesis and mitochondrial function (trichothecenes) (Marin et al. 2013). Xenoestrogens may have an immense impact on hormone homeostasis and endocrine disruption, especially in critical time windows, since they interfere with the endocrine system, partly even at extremely low concentrations (Xu et al. 2017; Sofie et al. 2014). Estrogenic chemicals occur for example naturally in plants (phytoestrogens) like genistein or daizein and synthetic estrogens

may be present in pharmaceuticals, insecticides and plasticizers (Paterni et al. 2017; Xu et al. 2017).

Similar to meaningful population-based metabolome research, also exposomics requires large-scale studies for exposome-wide association studies to draw reliable conclusions. The suggested mean sample size on male fertility was estimated to be 2700 men (Chung et al. 2019). Hence, high throughput methods are urgently needed as time is a limiting factor in large-scale epidemiological investigations. In the field of metabolomics, efforts to increase time efficiency are a current priority (Rampler et al. 2021; Liu et al. 2019). For example, the usefulness of a dual column approach to gain more information about the metabolome and lipidome within a short runtime was described by Schwaiger et al. (2019).

The combined and comprehensive measurement of the metabolome and the exposome is challenging as the concentrations of metabolites, drugs, food constituents and environmental contaminants span over estimated ten orders of magnitude and highly diverse classes of chemicals (Bloszies et al. 2018; Rappaport et al. 2014). Here, we present a rapid high-throughput workflow, combining the analysis of endogenous metabolites and multiple classes of xenobiotics in human urine and plasma. To cover polar compounds as well as the mostly non-polar xenobiotics, the approach utilizes a dual column approach with a reverse-phase (RP) and a hydrophilic interaction chromatography column (HILIC) being operated in parallel. To prove the power of the new method, the exposome coverage was evaluated based on more than 200 highly diverse analytes comprising endogenous metabolites and xenobiotics. The applicability to real-life samples was demonstrated by the analysis of urine samples of test sub-populations from Nigeria and Austria.

## MATERIALS AND METHODS

### Chemicals

A multi-analyte stock solution contained endogenous human metabolites (145 analytes) at 50  $\mu\text{M}$  and xenobiotics including estrogenic compounds (106 analytes) at a concentration between 5 – 5000 ng/mL (median 100 ng/mL) and was prepared in ACN/water (50/50; v/v) (Figure S1). In the context of this paper the estrogens are evaluated together with the xenobiotic substances and mentioned accordingly. In addition, 15 different isotopically labelled standards of xenobiotics and a separate  $^{13}\text{C}$ -labelled yeast extract (ISOTopic solutions, Vienna) were used as internal standards. A full list of all analytes is available in the Supporting Information (Table S1). A 24 h pooled urine sample obtained from a healthy female volunteer collected during one day after three days of a low xenoestrogen/polyphenol diet was chosen as model matrix in this study since urine is frequently used for assessing chemical exposure. Moreover, pooled human Li-Heparin plasma was acquired from Innovative Research (Novi, USA) as a second model matrix. Arylsulfatase/ $\beta$ -glucuronidase from *Helix pomatia* was purchased from Sigma-Aldrich (Vienna, Austria). All materials were stored at  $-80^\circ\text{C}$  prior to extraction. The concentrations of all analytes (xenoestrogens, mycotoxins and endogenous estrogens)

in the calibration standards (8 levels) are listed in the Supporting Information (Table S2). The remaining endogenous metabolites were present at concentrations between 0.001  $\mu\text{M}$  - 10  $\mu\text{M}$  at the same dilutions as the other analytes.

### Samples

For the optimization of the eluent/column combination a solvent standard and a matrix-matched standard at a medium concentration range (Level 6; Table S2) were used. SRM1950 (Metabolites in Frozen Human Plasma) and SRM3672 (Organic Contaminants in Smoker's Urine) were purchased from the National Institute of Standards & Technology (NIST, Gaithersburg, USA). In addition, 24 h urine samples from a food intervention study performed in 2021 with four different individuals (2 female and 2 male) collected at three different timepoints (3 different days) were tested. For details kindly refer to Oesterle et al. (2022). Furthermore, urine samples from Nigerian women sampled in 2016 were investigated. This longitudinal sample set was already analyzed before on biomarkers of mycotoxin exposure (Braun et al. 2022), therefore not all samples from the original study were available due to limited sample volumes. The sample set included 77 spot urine specimens from four timepoints (morning and evening over two days) of 23 mothers. All samples were stored at  $-80^\circ\text{C}$  until analysis.

### Sample preparation

During the whole sample preparation procedure, the samples were kept on ice. At first 200  $\mu\text{L}$  urine were mixed with 20  $\mu\text{L}$  internal standard mix (Table S3) and 20  $\mu\text{L}$  of the  $^{13}\text{C}$ -labelled yeast metabolite extract. For the experiment to determine the best solvent/column combination no internal standard was used, therefore only 40  $\mu\text{L}$  H<sub>2</sub>O were used instead of the internal standard mix. The samples were then vortexed. Afterwards, the samples were mixed with 760  $\mu\text{L}$  of extraction solvent (ACN:MeOH (1:1, v:v)). After thoroughly vortexing and sonication on ice (10 min), the samples were put on  $-20^\circ\text{C}$  for 2 h and centrifuged at 18,000 x g and  $4^\circ\text{C}$  (10 min) and 960  $\mu\text{L}$  of the supernatant was transferred to a new tube. Then, the samples were evaporated in a vacuum concentrator (Labconco). The residues were reconstituted in 192  $\mu\text{L}$  solvent (ACN/ water, 50:50, v:v), vortexed and centrifuged at  $4^\circ\text{C}$  for 10 min. Finally, the supernatants were transferred to HPLC vials and stored at  $-80^\circ\text{C}$  until analysis. Moreover, matrix matched calibration standards for urine and plasma were prepared by reconstituting matrix extracted according to the sample preparation protocol with respective solvent standard solutions. SRM3672 was additionally treated with a  $\beta$ -glucuronidase/arylsulfatase enzymes from *Helix pomatia* for 12 h at  $37^\circ\text{C}$  prior to extraction as the NIST certified reference values are given for deconjugated samples. This additional step was not performed for the other samples because the heat treatment would have disturbed measurements of endogenous metabolites. A non-deconjugated sample was prepared for the SRM material for comparison as well.

### Quality control measures

As quality control samples, SRM 1950 in one to ten dilution and a solvent QC comprising all target analytes at 1  $\mu\text{M}$  (metabolites) and

approximately 100 ng/mL (xenobiotics) were analyzed throughout the sequence. Moreover, separate pooled urine samples from the measured Nigerian and Austrian were repeatedly injected with a maximum of nine samples between the injection of the pooled urine samples to check the instrument performance. Solvent blanks (pure reconstitution solvent) and system blanks (200  $\mu$ L water extracted according to the sample preparation protocol) were measured to correct for contaminations in the system and during the sample preparation.

### LC-HRMS(/MS) analysis

To optimize chromatographic separation for our highly diverse set of endogenous and exogenous analytes, a Vanquish Duo UHPLC system with two independent pumping systems and two different columns was used. Different column/eluent systems were examined. As reverse-phase column (RP), an Acquity HSS T3 (1.8  $\mu$ m, 100 x 2.1 mm) was used. For HILIC chromatography, two different hydrophilic interaction liquid chromatography columns (HILIC) were used, namely, a SeQuant<sup>®</sup>ZIC<sup>®</sup>-pHILIC (5  $\mu$ m, polymeric, 150 x 4.6 mm) and an Acquity BEH Amide (1.8  $\mu$ m, 100 x 2.1 mm) were tested. Eluent B was in all cases 100% ACN. The aqueous eluent (solvent A) was changed as stated in Table 1. The injection volume was 5  $\mu$ L for all columns and experiments.

For the RP measurements the gradient was as follows: 0 - 1 min, constant flow at 10% B; 1 - 10 min, increase to 70% B; 10 - 11 min, rise to 100% B and 13.5 - 15 min, equilibration at 10% B. A hydrophilic interaction liquid chromatography column (HILIC), SeQuant<sup>®</sup>ZIC<sup>®</sup>-pHILIC (5  $\mu$ m, polymeric, 150 x 4.6 mm) was operated with the following gradient: 0-1 min, constant flow at 75% B; 1-6 min, linear decrease to 50%; 6-7 min, drop to 30% B; 7-11 min, constant follow at 30%; 11-15 min, equilibration at 75% B. Both columns were at 40 °C and a flow rate of 0.3 mL/min was set. The Acquity BEH Amide was operated with a slightly different gradient as follows: 0-2 min, constant at 80% B; 2-8 min decrease to 40% B; 8-10 min, constant at 40% B and 10-15 min, equilibration at 80% B. Both capillaries were connected with a T-piece to mix the effluents before introduction into the ESI source of the mass

spectrometer (Figure 1A). As needle wash, 75% ACN was used for the HILIC measurement, while for the RP run H<sub>2</sub>O:ACN:MeOH (2:1:1,v:v:v) was applied.

Measurements were conducted in fast polarity-switching full scan mode on a Q Exactive HF quadrupole-Orbitrap mass spectrometer. The settings of the ESI interface were as follows: sheath gas, 48 au; auxiliary gas, 11 au; sweep gas flow, 2 au; capillary voltage, 3.5 kV (positive), 2.8 kV (negative); capillary temperature, 260°C; auxiliary gas heater, 410°C. The scan range was from 65 to 900 m/z. For full scan only measurements the resolution was set to 60,000 with an AGC target (automatic gain control) of 1 x 10<sup>6</sup> and a maximum injection time of 200 ms. The instrument was calibrated before the analysis.

Following the optimization of chromatographic conditions, the most suitable RP/HILIC combination was selected, consequently the above-mentioned parameters of combination two (Figure 1B) were applied for the sample measurement. A mixture of both effluents entered the mass spectrometer via the ESI source (Figure 1C). For analyses with data-dependent MS<sup>2</sup> a resolution of 60,000 with an AGC target of 1x10<sup>6</sup> and a maximum injection time of 100 ms were chosen for the full scan. The settings for the MS<sup>2</sup> collection were the following: resolution, 30,000; AGC target, 1 x 10<sup>5</sup>; maximum injection time, 50 ms, loop count, 10; isolation window, 1.0 m/z; normalized collision energy, 30 eV; minimum AGC, 8x10<sup>3</sup>; dynamic exclusion, 4 s. Iterative exclusion lists were generated with IE-Omics (Koelmel et al. 2017). The urine samples from Nigeria and Austria were analyzed in randomized order.

### Data Analysis

Skyline (version 20.2.0.286, (MacLean et al. 2010)) was used for targeted analysis and quantification. Internal standard correction was performed. If for the specific analyte no internal standard was included, the internal standard with the closest retention time was selected as surrogate standard for normalization (Table S7). The linear calibration curves (Table S7) were 1/x weighted. Matrix matched calibration for urine and plasma was performed and the

**Table 1** Optimization design of the tested column/eluent systems for the dual approach

	Combination 1	Combination 2	Combination 3	Combination 4
<b>RP</b>				
Column	Acquity HSS T3			
Aqueous eluent	0.6 mM NH <sub>4</sub> F in H <sub>2</sub> O	0.3 mM NH <sub>4</sub> F in H <sub>2</sub> O	1 mM NH <sub>4</sub> F in H <sub>2</sub> O	0.6 mM NH <sub>4</sub> F in H <sub>2</sub> O
Organic eluent	ACN			
<b>HILIC</b>				
Column	SeQuant <sup>®</sup> ZIC <sup>®</sup> -pHILIC		Acquity BEH Amide	
Aqueous eluent	10 mM NH <sub>4</sub> HCO <sub>3</sub> (pH 9.2) in H <sub>2</sub> O /ACN (9:1, v:v)	2 mM NH <sub>4</sub> F in H <sub>2</sub> O	1 mM NH <sub>4</sub> F in H <sub>2</sub> O	50 mM CH <sub>3</sub> COONH <sub>4</sub> (pH 6) in H <sub>2</sub> O
Organic eluent	ACN			

corresponding calibration curves were used for quantification of xenobiotics. However, endogenous metabolites were, as expected, frequently highly abundant in the matrices, therefore solvent calibration was applied for endogenous metabolites (excluding estrogens). Limit of detections (LODs) were determined based on

the EURACHEM guideline (Ellison et al. 2012) as three-times the standard deviation of the multiple injection of a low-concentrated standard (n=6) divided by the square-root of the number of replicates. For the limit of quantification (LOQ) the tenfold standard deviation was used.

Spearman correlation was calculated for compounds positive in at least 20% of all Nigerian samples with R and plotted with the *corrplot* package (version 0.90) (Wei et al. 2017). For pathway analysis MetaboAnalyst 5.0 (Pang et al. 2021) was used. A hypergeometric test was selected as enrichment method and for topology analysis relative-betweenness centrality. The pathway library was *Homo sapiens* (KEGG).

The pooled Nigerian urine sample including MS2 data measured in negative and positive ionization mode with iterative exclusion lists (n=4) was used to screen for potential additional xenobiotics not covered by the targeted evaluation using authentic reference standards. Suspect screening was performed in R applying the

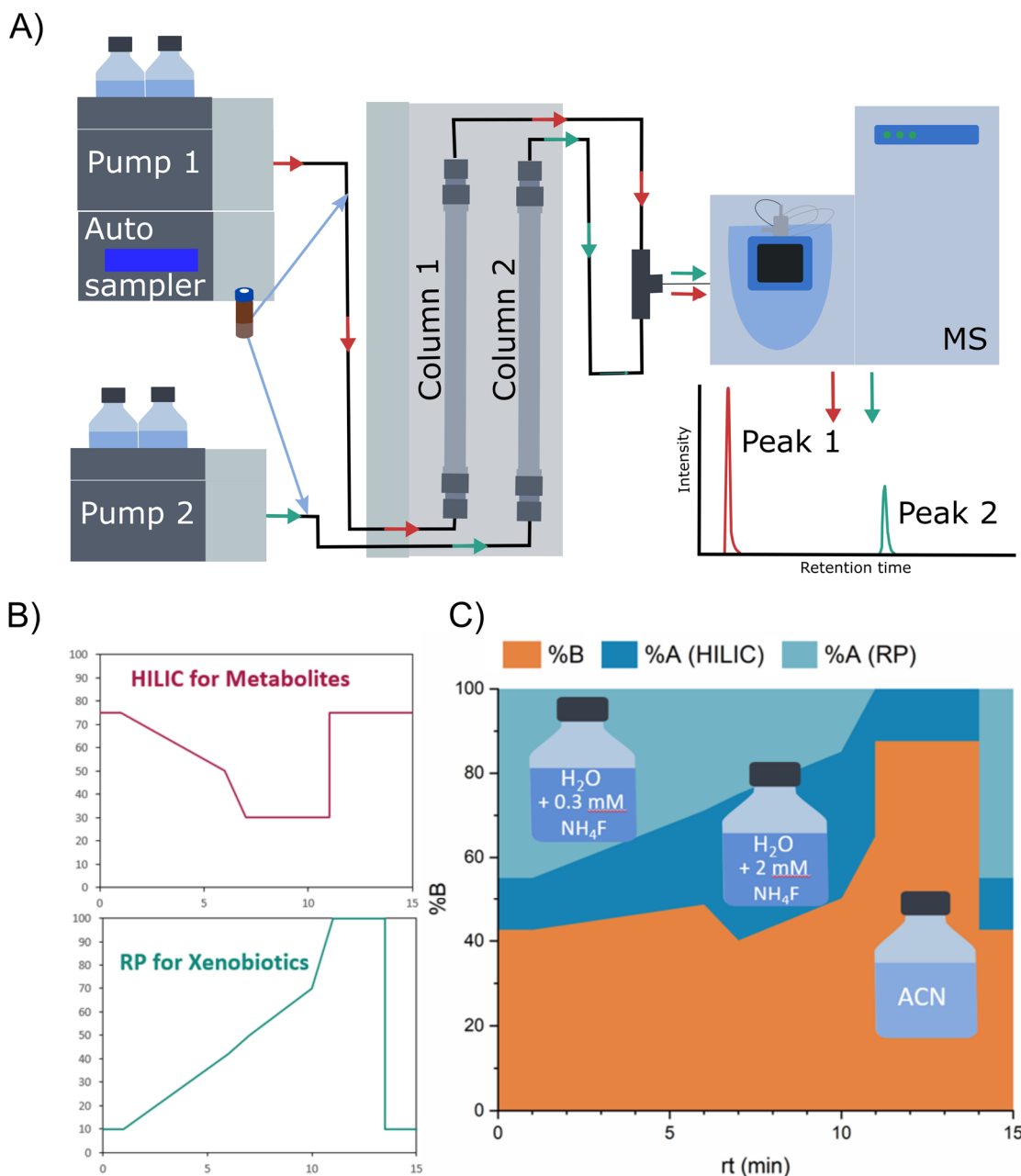


**Figure 1** Dual column setup (A) LC-HRMS system comprising two separate LC-pumps and columns combined by a T-piece before entering the mass spectrometer. (B) Gradients of both individual columns. (C) Eluent composition entering the mass spectrometer after the effluents were mixed

patRoan package (Helmus et al. 2021). Solvent blanks (only in the corresponding polarity) were defined as blank measurements. The raw data files were converted to mzML-files and centroided with ProteoWizard (Chambers et al. 2012). For peak picking and grouping the "openms" algorithm was set with the following

parameters: noise threshold: 4E3, chromFWHM: 3, minFWHM: 1, maxFWHM: 30, chromSNR: 5 and mzPPM: 3. Only features with a minimum absolute feature intensity of 3E5, a minimum feature intensity above blank of 10, present in at least 60% of replicates were kept and blank analyses were removed after this step. A

suspect list from the ENTACT trial (Sobus et al. 2019) based on the EPA's ToxCast library including > 4000 substances was adopted for this experiment. Analytes which had already been included in the targeted list were removed to avoid redundancy. For the suspect screening a m/z window of 0.002 was set. MS peak list data was extracted with the mzr-algorithm (precursor m/z window: 0.5) and filtered (relative intensity threshold: 0.02, top 10 MS/MS peaks). Then molecular formulas were generated considering [M+H]<sup>+</sup> and [M-H]<sup>-</sup> adducts respectively and the elements C, H, N, O, P, S, Cl, Br using genform. Chemical compounds were annotated with metfrag and the comptox database. With annotateSuspects and the generated peak lists, formula and compound data the suspect screening results were refined. An identification level was assigned depending on the rank and scores (isoScore, individualMoNAScore) of formula/compound candidates roughly based on Schymanski et al. (2014). The default settings in the annotateSuspects algorithm were applied. As no retention time data was available, level one identifications were not possible. The other identification levels were: level 2a (good MS/MS library match, top ranked in compound results, individualMoNAScore  $\geq$  0.9, no MoNA library score for other candidates), level 3a (fair library match, individualMoNAScore  $\geq$  0.4), level 3b (known MS/MS match, at least three fragments match), level 3c (good in-silico MS/MS match, annotation MS/MS similarity (annSimComp)  $\geq$  0.7), level 3c (good formula MS/MS match, top ranked formula candidate, annSimForm  $\geq$  0.7, isotopic match (isoScore)  $\geq$  0.5, both scores at least 0.2 higher than next best ranked candidate), level 4b (good formula isotopic pattern match, top ranked formula candidate, isoScore  $\geq$  0.9, score at least 0.2 higher than next best ranked candidate) and level 5 (nothing of the above mentioned criteria match).

## RESULTS & DISCUSSION

### Establishing a dual column approach for combined exposure & effect analysis

#### Selection of columns and eluents

In optimization experiments different eluent-column combinations were tested for the best overall performance and compatibility. Only eluents with a basic (pH 9.2) to slightly acid pH (pH 6) were combined with NH<sub>4</sub>F to avoid the formation of hydrofluoric acid. For a representative selection of selected compounds (25 metabolites on the HILIC column and 25 xenobiotics on the RP column) the averaged peak area (n=4-6) in a matrix-matched standard (urine) and a solvent standard both at a medium concentration level (level 6) were compared between the combinations (Figure 2 and Table S4). Peak areas were normalized to the best combination for each analyte to simplify comparison. Endogenous metabolites are naturally abundantly present in urine, therefore the peak areas in the standard-spiked urine were increased compared to the solvent standards. For xenobiotics, the observed signal was mostly decreased due to signal suppression in the urine matrix. The averaged peak areas of the selected

metabolites showed that the combination of 2 mM NH<sub>4</sub>F/ACN on a SeQuant<sup>®</sup>ZIC<sup>®</sup>-pHILIC column (HILIC) and 0.3 mM NH<sub>4</sub>F/ACN on an Acquity HSS T3 is favourable (highest peak area) in solvent. However, the difference to the three others is only minor with combination 2 reaching about 85% of the average peak area of combination 1. In urine, the average peak area of combination 4, which uses an Acquity BEH amide column instead of a SeQuant ZIC-pHILIC column, is only about half of the others. Except for combination 4, all eluent-column combinations performed similar, but with combination 2 and 3, both using NH<sub>4</sub>F as additive, up to four metabolites (choline, phosphocreatinine, citric acid, 3-methylcytidine) were not detectable at the chosen concentration level, therefore the SeQuant ZIC pHILIC column with a basic NH<sub>4</sub>CO<sub>3</sub> buffer based on Schwaiger et al. (2019) seemed to be the best choice regarding endogenous metabolites excluding estrogen hormones. When xenobiotics and endogenous estrogens were investigated, however the additive NH<sub>4</sub>F clearly outperformed the basic buffer. The average peak area in urine and solvent of this group nearly doubled when NH<sub>4</sub>F was used. Since xenobiotics are generally less concentrated than metabolites in real-life samples, we decided to use this additive to boost their sensitivity and finally selected the combination with 2 mM NH<sub>4</sub>F as aqueous HILIC eluent and 0.3 mM NH<sub>4</sub>F as aqueous RP column due to a better overall performance.

#### Long term stability of LC-MS setup

A solvent QC sample containing endogenous metabolites at 1  $\mu$ M and xenobiotics at approximately 100 ng/mL was injected throughout the sequence (n=11) spanning over a period of 40 h. Only the most abundant ion species was considered. For endogenous metabolites the peak from the HILIC column and for xenobiotics the peak from the RP column was evaluated. At the chosen concentration level, 113 out of the 146 metabolites (77%) retained with a retention time bigger than 1 min on the HILIC column and 104 out of the 106 xenobiotics (98%) with retention on the RP column (retention time > 0.8 min) were detectable. Four analytes were not detectable even at higher levels, therefore the best ionization mode remains unclear. The relative standard deviation (RSD) was calculated for the peak area and the retention of all detectable molecules at this level (Figure 3A and 3B). The median RSD of the area was 21.7% and 31% in negative and positive ionisation mode, respectively. The difference between peaks from the HILIC and RP separation was minor, but in positive ionisation mode the relative standard deviation was bigger. Regarding retention time the median RSD was 0.4% for negative mode and 0.7% for positive mode. The xenobiotics' retention times were more stable with a median of 0.3% compared to 1.3% for the endogenous metabolites.

The recoveries ranged in solvent between 83% and 123% with an average of 104% for xenobiotics and 81% and 119% with an average

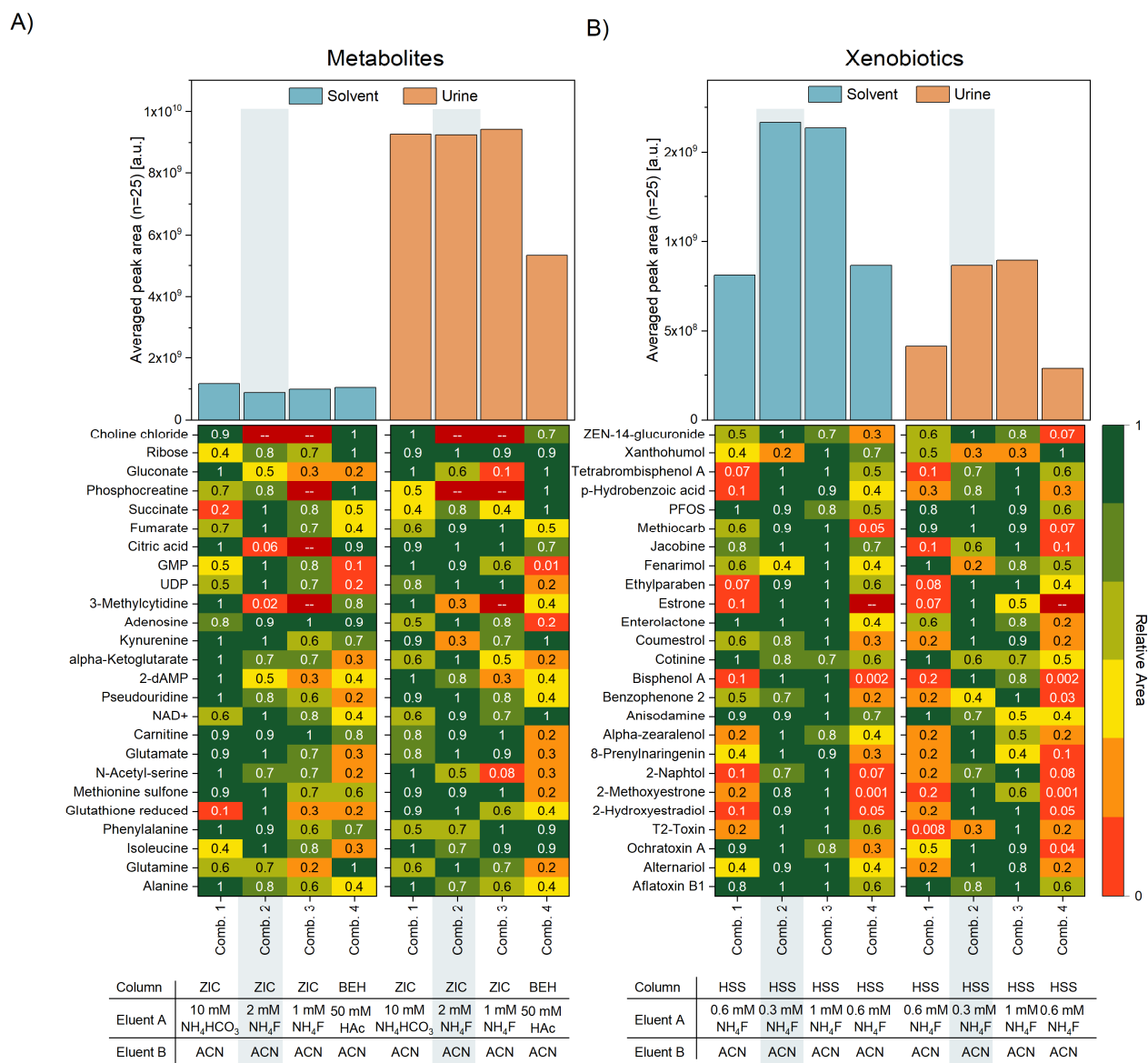


**Figure 2** Comparison of the average peak areas of selected, representative endogenous metabolites (A) and xenobiotics including estrogen hormones (B) in solvent and urine including a detailed overview of the averaged peak areas (n=4-6) relative to the highest peak area of the individual molecule. The best combination is shaded in grey. Different columns, namely Acquity HSS T3 (HSS), SeQuant<sup>®</sup>ZIC<sup>®</sup>-pHILIC (ZIC), Acquity BEH Amide (BEH), and eluents, namely 0.3/0.6 /1/2 NH<sub>4</sub>F in H<sub>2</sub>O (0.3/0.6/1/2 mM NH<sub>4</sub>F), 10 mM NH<sub>4</sub>HCO<sub>3</sub> (pH 9.2) in H<sub>2</sub>O/ACN (9:1, v:v) (10 mM NH<sub>4</sub>HCO<sub>3</sub>), 50 mM CH<sub>3</sub>COONH<sub>4</sub> (pH 6) in H<sub>2</sub>O (50 mM HAC) were tested

of 101% for endogenous metabolites (Table S19/Table S20). Furthermore, the extraction recoveries were evaluated in spiked urine and plasma samples. The median recovery of xenobiotics was 97% in urine and 103% in plasma whereas for metabolites these figures were determined to be 97% and 99%, respectively. Only 10% of the analytes in urine and 14% in plasma, had a recovery below 80%. The recoveries were above 120% for about 1% of compounds in urine and 3% in plasma. Several analytes, especially endogenous metabolites, were already present in high quantities

in the non-fortified urine and plasma, hence the extraction recovery was not estimated for all compounds.

Pooled quality control samples of both sample sets were measured several times throughout the measurement (Figure S2). The relative standard deviation of the retention time and the normalised peak area was calculated for highly diverse analytes. This included Bisphenol A (BPA), daidzein, enterodiol, glycitein, methylparaben and triclosan in the pooled urine of the Nigerian samples (n=9) and BPA, daidzein, nonylphenol and p-

hydroxybenzoic acid in the pooled urine of the Austrian samples (n=5). In addition, four metabolites (tryptophan, uracil, fumaric acid, gluconate) were investigated. The relative standard deviation of the retention time was < 1.5% for all analytes except fumaric acid (about 2.8%). The relative standard deviation of the normalised area was < 20% for all analytes except for BPA (22%), which was only at a concentration around the LOD in the Austrian pooled urine sample. The variation tended to be lower if the corresponding <sup>13</sup>C-labelled compound was available for compound-specific internal

standardization (e.g. for methylparaben) as compared to surrogate internal standardization.

#### Quantification of reference material

The limits of detection for the xenobiotics ranged from 0.01 to 5.7 ng/mL with a median of 0.08 ng/mL in solvent (Table S5, Figure 4C). In matrix the median LOD increased to 0.7 (urine, Figure 4A) and 0.5 (plasma, Figure 4B) most likely due to matrix effects and matrix interferences. Phytoestrogens like daidzein

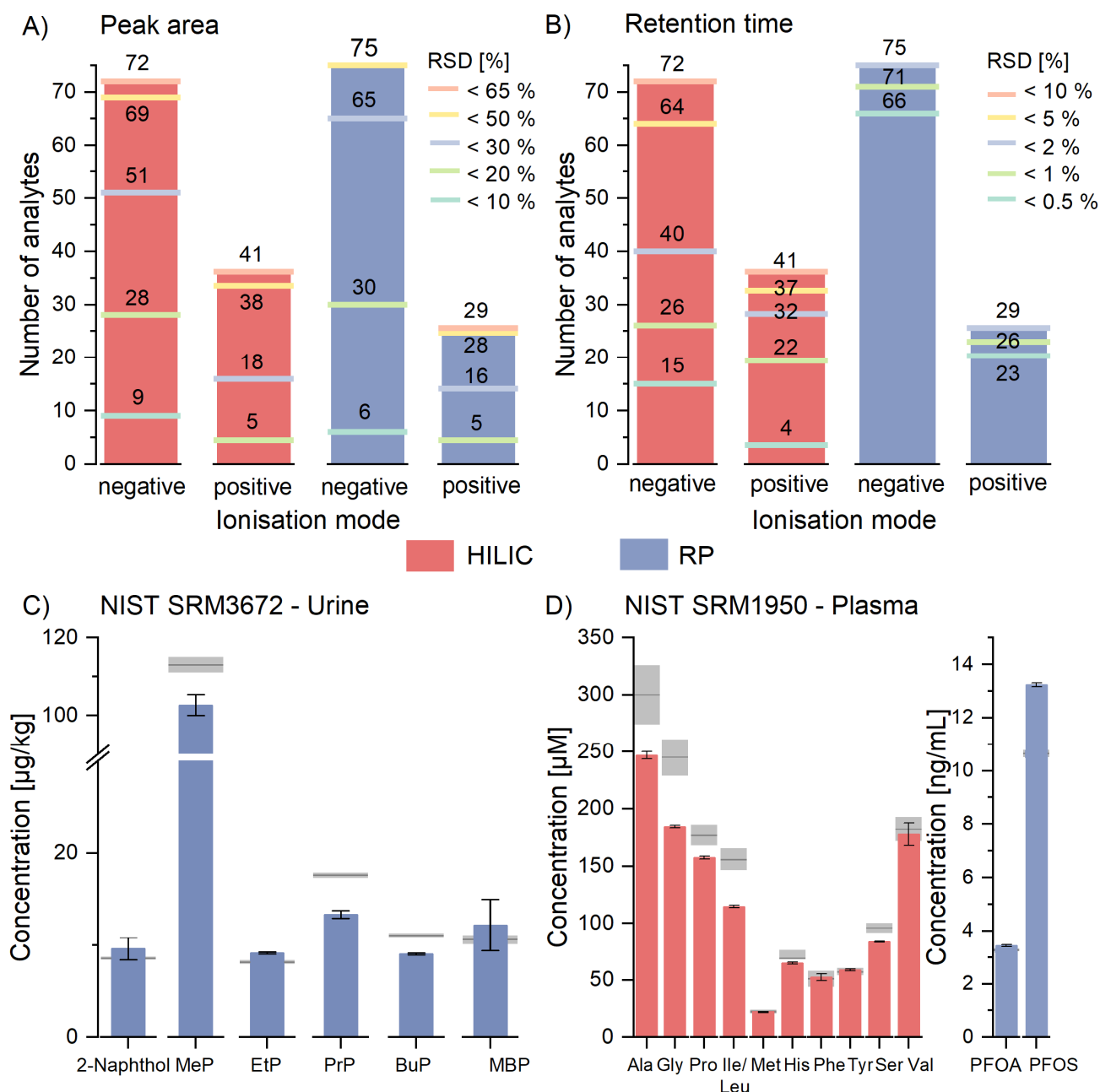


**Figure 3** Repeatability and accuracy reported as the number of analytes within a certain relative standard deviation of A) peak area and B) retention time. The lines mark the thresholds and the labels indicated how many analytes fall below a respective RSD percentage. Only the most abundant ion species was considered on the respective column. C) Analytes reported in SRM3672 and D) in SRM1950 with the grey line indicating the certified reference value and the expanded uncertainty according to the certificate of analysis

and genistein and personal care product ingredients e.g., parabens exhibited the lowest LODs. The LODs were for most xenobiotics sufficient to detect them in averagely contaminated samples considering concentration levels from published human biomonitoring studies. For example, published paraben levels in urine exceed 100 ng/mL for methylparaben and 20 ng/mL for propylparaben in several human biomonitoring studies (Wei et al. 2021), which is more than 100-times the LOD value of the reported method. The analysis of bisphenol levels in U.S. urine samples showed levels of 0.4 -2 ng/mL BPA, 0.15-0.5 ng/mL BPF and <0.1-0.25 ng/mL BPS (Ye et al. 2015), making the detection of BPS and BPF difficult, but BPA was detected at a concentration above our method's LOD. Mycotoxins were reported to be present in Nigerian urine samples at an average concentration of 0.75 ng/mL (ZEN) and 0.06 ng/mL (AOH) (Šarkanj et al. 2018). The average levels of these mycotoxin were just slightly above our calculated LOD. However, these toxins would be detectable in medium to highly contaminated samples. For triclosan mean concentrations of 28.6 ng/mL were detected in urine from the USA, Greece, and Asian countries (Iyer et al. 2018). In Israeli urine the mean detected concentration was 28.9 ng/mL for monobutyl phthalate, 12 ng/mL for MEHP, 0.17 ng/mL for 1-OH pyrene, 26.9 ng/mL for genistein and 66.8 ng/mL for daidzein (Berman et al. 2013). Besides 1-OH-pyrene, the pesticide triclosan, plasticizers and phytoestrogens were reported in concentration ranges covered with our approach. The linear dynamic range was highly variable and depended on the molecule (Table S19). About 10% of the xenobiotics had a linear range spanning five orders of magnitude. Half of them covered a range of four, and approximately a third a range of three orders of magnitude in solvent. Matrix-matching resulted typically in a reduction of the dynamic range of about one order of magnitude due to matrix effects as the LOD of the xenobiotics in matrix was generally lower.

The solvent LOD of endogenous metabolites ranged from 0.001  $\mu\text{M}$  to 6.6  $\mu\text{M}$  with a median of 0.04  $\mu\text{M}$  (Table S6, Figure 4D). The LOD values were estimated for 134 analytes including several jointly evaluated isomers. The LOD of several endogenous metabolites was not estimated in the human matrices due to their high natural abundance. About one third of all compounds showed LODs < 0.01  $\mu\text{M}$  and about two thirds < 0.1  $\mu\text{M}$  allowing for the straight-forward (semi-) quantitative assessment of the metabolome in most biological systems. The reference standards spanned five orders of magnitude from 0.001  $\mu\text{M}$  to 10  $\mu\text{M}$ . However, most metabolites were not detectable at the lower calibration level (0.001  $\mu\text{M}$  – 0.01  $\mu\text{M}$ ) limiting the linear dynamic range to four (45%), three (29%) or even less (8%) orders of magnitude (Table S20).

### Limitations

Out of the 146 endogenous metabolites present in the standard mix, five (1-methylnicotinamide, thiamine, choline, spermine and

spermidine) were not detectable even at the highest concentration level (10  $\mu\text{M}$ ). Isomers were not separated in some cases. These included 2-/3-phosphoglyceric acid, citric /isocitric acid, homoserine/threonine and isoguanosine/guanosine. The hexoses fructose, galactose, mannose, glucose and inositol were not distinguishable as well as their phosphates (fructose-6-phosphate, glucose-1-phosphate and glucose-6-phosphate) as they were co-eluting and therefore the peaks were not baseline separated. Pentose-phosphates, ribose-5-phosphate and ribulose-5-phosphate were not baseline separated, too. For arginine and palmitic acid no satisfactory linear regression was possible most likely due to severe carry-over effects.

Six analytes for which certified reference values are available in SRM3672 (Organic Contaminants in Smoker's Urine) were detected and quantified (Table S13). As the values stated in the certificate were total analyte concentrations after hydrolysis,  $\beta$ -glucuronidase/arylsulfatase-treated reference urine was analyzed. The relative error compared to the reference value was < 20% for all of these (Figure 3C). 1-OH-pyrene and MEHP were not detected, although they are present in the smokers' urine due to their low concentration below the method's quantification limits. Besides several amino acids, PFOA and PFOS were quantified in SRM1950 (Metabolites in Frozen Human Plasma) and compared to the certificate (Figure 3D, Table S14). Threonine was not evaluated as it coeluted with homoserine and therefore only a combined value for both amino acids was available. Isoleucine and leucine were not baseline separated as well, but for both molecules reference values were given, therefore the sum of both concentrations was compared. The relative error was < 26% for all amino acids, whereby the recoveries were in general lower for the high abundance amino acids (glycine (75%), alanine (82%), isoleucine/leucine (74%)), possibly due to saturation effects as the values were outside of the calibration range (Figure 3D). The samples were injected undiluted to ensure a high detectability of low-concentrated xenobiotics despite possible saturation issues for the endogenous metabolites at higher concentrations. The relative errors of PFOA and PFOS were even < 5% and < 20%, respectively. In general, the determined values were in good agreement with the reference values of both SRMs especially given the extremely broad scope of the new workflow with recoveries ranging from 74% to 124% in SRM1950 and recoveries between 81% and 115% in SRM3672 (Figure 3C). These recoveries are similar to values reported in literature for SRM3672 by Karthikraj et al. (2020) (80.5% - 105%) and Zhu et al. (2021) (80 – 111%).

In the reference materials, several additional metabolites and xenobiotics were quantified (Figure S3, Table S16). In SRM3672, 18 xenobiotics and two estrogens were detected. SRM1950 was contaminated with 17 xenobiotics with nine of them being detected in both reference materials including personal care



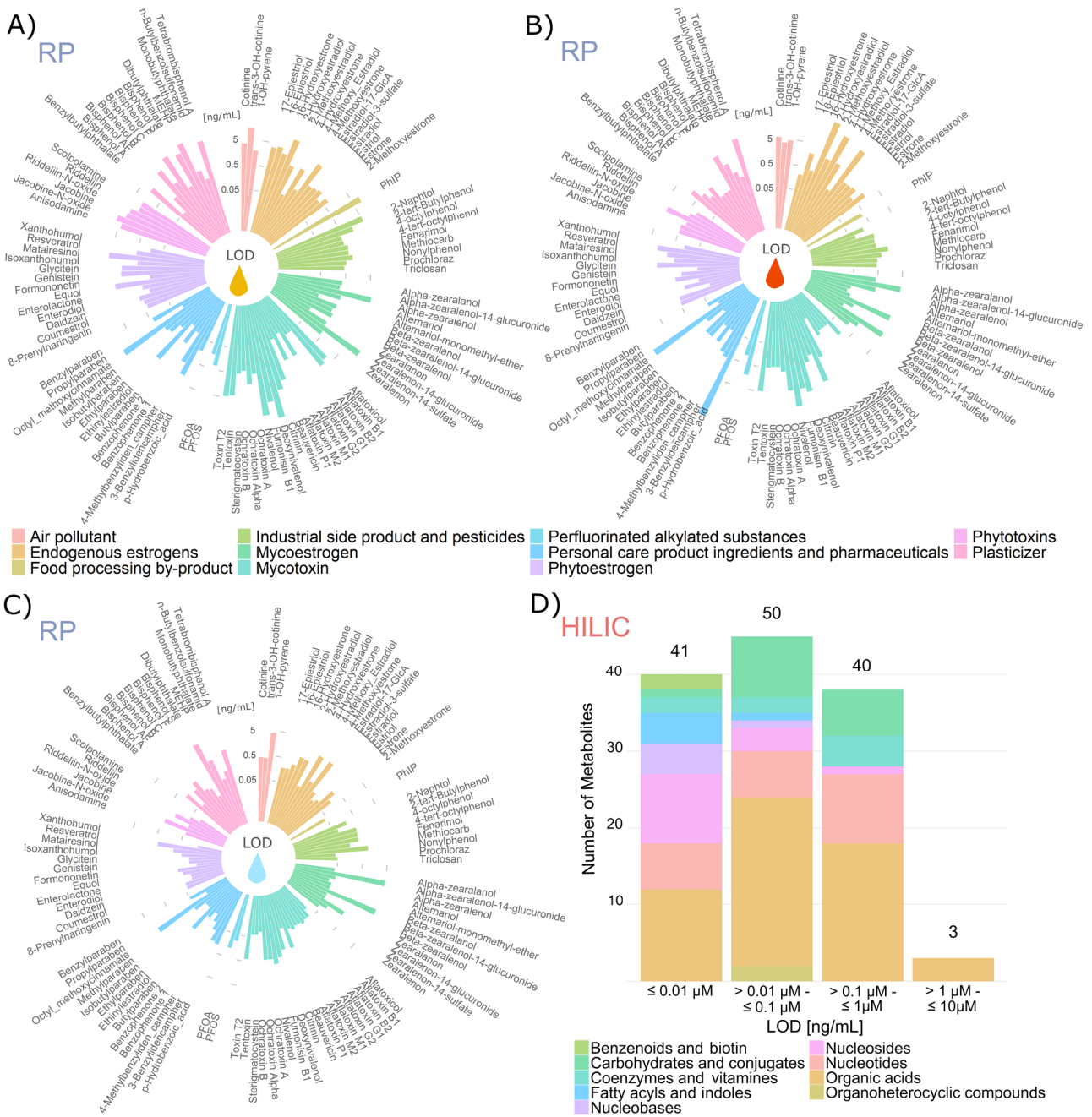


**Figure 4** Limit of detection (LOD) of representative xenobiotics and estrogens in urine (A), plasma (B) and neat solvent (C) sorted by compound classification. The values were plotted on a logarithmic scale. D) Number of endogenous metabolites in a specific LOD range. The colour indicates the category to which the analytes can be classified to

product ingredients (methylparaben, propylparaben, p-hydroxybenzoic acid, benzophenone-1), phytoestrogens (genistein, daidzein), smoking markers (cotinine, trans-3-OH-cotinine) and an industrial side product (2-naphthol). In SRM3672 additional phytoestrogens (e.g. enterolactone, enterodiol, daidzein, glycitein), a plasticizer (mono butyl phthalate) and butylparaben were observed, whereas in SRM1950 scopolamine, a phytotoxin, perfluorinated substances (PFOA, PFOS), industrial side products (nonylphenol, 4-tert-octylphenol) and other plasticizers (BPS, BPA) were found. The quantified metabolome comprised 48 (SRM1950)

and 61 (SRM3672) additional compounds, respectively. Smoker's urine was not enzyme treated for the evaluation. Mainly amino acids, nucleobases and nucleosides were quantified in these samples. The concentrations ranged over four orders of magnitude for metabolites in the urine plasma reference material. When expanding to exogenic contaminants this range spanned even over six orders of magnitude. In the urine reference material concentrations were less variable covering three orders of magnitude.

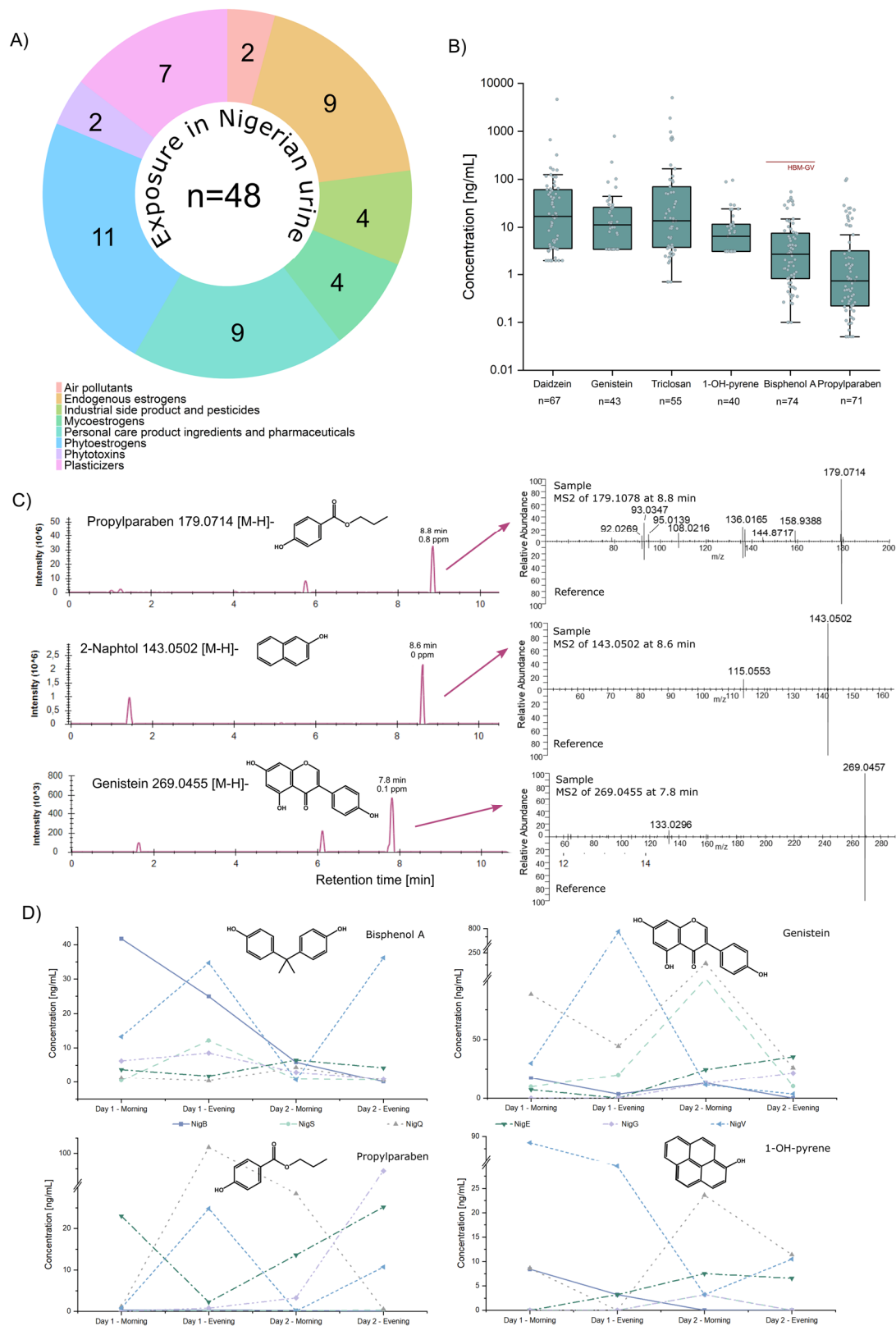


**Figure 5** Detection of xenobiotics in Nigerian samples. A) Variety of observed xenobiotics and their classification. B) Individual concentrations of selected analytes that have been detected in > 50% of the samples (n=77). The human biomonitoring (HBM) guidance value (Ougier et al. 2021) was added in red. C) Extracted ion chromatograms (XICs) of selected analytes including corresponding MS2 spectra of experimental samples and authentic reference standards. D) Variation of analyte concentration in six individuals for selected xenobiotics demonstrate severe exposure dynamics and the need for longitudinal sampling design

## Application in biomonitoring studies from Europe and Sub-Saharan Africa

The established analysis pipeline was applied in proof-of-principle studies of two different urine sample sets from geographically different areas, Austria and Nigeria. Both studies included several individuals (Austria (4) and Nigeria (23)), who donated samples at four different time points. In the Austrian samples 17 different xenobiotics belonging to four compound categories were identified (Figure S5A/B, Table S10). Most exposures were either personal care product ingredients or phytoestrogens. The Nigerian urine samples were contaminated with more than twice as many chemicals ( $n=48$ ) coming from diverse sources (Figure 5A, Table S9), but personal care product ingredients and phytoestrogens were still the dominant classes. Concentrations covered five orders of magnitude from the sub-ppb to the ppm range. The Nigerian samples were contaminated with a wider diversity of chemicals including air pollutants (1-OH-pyrene), mycoestrogens (ZEN, AME) and industrial side products (2-naphthol) and higher concentration levels. In particular the maximum values were frequently 10-100-times higher compared to the Austrian samples. However, especially the Austrian dataset was small and homogenous, therefore the available data is not sufficiently representative to estimate population-wide exposure levels. The Austrian samples were considered as low-exposure scenario, whereas the Nigerian samples were regarded as high-exposure samples as often food/environmental safety regulations are lacking or not adequately enforced. Each detected xenobiotic was on average detected in 31 out of 77 Nigerian samples. Four analytes (enterolactone, BPA, nonylphenol and propylparaben) were present in >90% of all samples (Figure 5B). In the Austrian samples, two thirds were contaminated with daidzein, 4-tert-octylphenol, BPA and propylparaben, besides the in all samples detected nonylphenol and dibutyl phthalate. MS2 spectra further supported identification (Figure 5C), although for all analytes discovered here reference standards were used for retention time confirmation. The number and level of the detected phytoestrogens was restricted due to the regulated diet with no vegetable and fruit intake except for a smoothie on day 2 before the Austrian study and on the first two study days. Approximately 70 diverse endogenous metabolites were quantified in the urine samples of both studies (Table S11, Table S12). Thirteen individuals completed the full longitudinal sampling with four timepoints. The variation over the timeframe of two days is exemplary depicted for six individuals and analytes of distinct origin including the plasticizer bisphenol A, the phytoestrogen genistein, the personal care product ingredient propylparaben and the air pollutant 1-OH-pyrene in Figure 5D. The concentrations spanned over three orders of magnitude within the sample individual. Genistein and propylparaben differed vastly between the timepoints in particular. The intraindividual variation was like the interindividual variation demonstrating the importance of longitudinal sampling for exposure assessment for several participants. The diversity and high dynamic of the exposome even within the same individual was described previously (Jiang et al. 2018) and further supports the need for time-resolved testing to capture dynamic exposure in spot urine samples or 24 h urine.

To showcase the power of our approach for investigating the impact of exogenous exposures on the endogenous metabolite, a

spearman correlation matrix was created. Various significant correlations between xenobiotics but also xenobiotics and metabolites were demonstrated (Figure S4). Mainly analytes which were detected in a multitude of samples, e.g., mono butyl phthalate, ethyl paraben, MEHP, benzophenone and enterolactone, yielded significant correlations, probably due to the higher statistical power. High correlation coefficients were observed for monobutyl phthalate and MEHP (0.72), ethyl paraben and p-hydroxybenzoic acid (0.64), benzophenone-1 and enterolactone (0.74), and propylparaben and methylparaben (0.59). MEHP and monobutyl phthalate are both urinary biomarkers of phthalate exposure with estrogenic potential (Wenzel et al. 2018). The preservatives ethyl paraben and p-hydroxybenzoic acid were likely to be an ingredient in the same type of personal care products and also methylparaben and ethyl paraben may be present in similar products. Enterolactone, a biotransformation product of plant lignans originating from e.g. flaxseeds and sesame (Axelson et al. 1982), and the urinary biotransformation product of benzophenone-3, benzophenone-1, a UV-filter used in cosmetics (Kang et al. 2019), clearly have different sources. However, both are hormonally active and have a shared mechanism concerning obesity antagonism. This was demonstrated to be associated with late on-set of puberty in girls (Wolff et al. 2015).

The link between external exposures and the ensuing disturbance of the internal metabolome is one step to elucidate disease development, which is part of the broad scope of exposome research. With our approach connections between xenobiotics and metabolites were indicated. A strong correlation between ethyl paraben and the carboxylic acids fumaric acid (0.68) and malic acid (0.67) and the amino acid alanine (0.62) were uncovered. Alanine (0.64), fumaric acid (0.63) and malic acid (0.6) were connected to benzophenone-1, too. The matrix also strongly correlated mono butyl phthalate and aspartic acid (0.66).

Phthalate exposure was associated with altered carnitine levels and changes in metabolites associated with amino acid metabolism in urine of Chinese men (Zhang et al. 2016). In our study, carnitine, propionylcarnitine and several amino acids were correlated with mono butyl phthalate, too. Pathway analysis was performed for significantly correlated metabolites with mono butyl phthalate (Figure S6). The results revealed a strong impact on the alanine, aspartate and glutamate metabolism, the arginine biosynthesis, and the citrate cycle. The pathway analysis of with ethyl paraben associated metabolites exposed similar results with arginine biosynthesis and alanine, aspartate and glutamate metabolism being the most impacted pathways (Figure S7). These two pathways were also the most affected among with benzophenone-1 correlated metabolites (Figure S8). The xenobiotics benzophenone-1, mono butyl phthalate and ethyl paraben had at least a moderate correlation (correlation coefficient between 0.5 and 0.64) among each other, therefore the disturbance in amino acid metabolism might not be triggered by a single compound but rather by a mixture of different chemicals.

Recent studies demonstrated the feasibility of exposome-wide association studies (ExWAS), e.g. extensive effect biomarker and biomarker discovery of air pollutant exposure (Tang et al. 2021) and linking metabolic profiling and exposure to perfluoroalkyl

substances (Alderete et al. 2019). However, to capture the metabolome and the chemical exposome several independent measurements were required, increasing the measurement time compared to our 15 min LC-HRMS/MS run covering both polar metabolites and the primarily apolar xenobiotics. Especially molecules with a high vapor pressure and low boiling/melting point were not accessible with LC-MS technology, therefore GC-MS would need to be integrated to further extend coverage (Ulrich et al. 2019; Hu et al. 2019). Although our fast LC-MS approach might be advantageous regarding run time, the vast concentration difference between endogenous metabolites and environmental contaminants (Bloszies et al. 2018) hamper their simultaneous measurement as several endogenous metabolites were close to the detector saturation and low abundant xenobiotics still need higher sensitivity. In particular, quantification posed a challenge, as calibration ranges were partially exceeded. Internal standard correction eased linearity issues especially at high concentrations.

### Suspect screening in biological samples obtained from Nigerian women

To demonstrate the workflow's suitability for suspect and non-targeted screening/analysis (NTS/NTA), raw data from four pooled Nigerian urine samples with iterative MS2 exclusion lists were processed for suspect screening. On average 14,126 and 18,408 features were picked in each sample in negative mode and positive mode, respectively. 16,288 negative features in 4,590 groups remained after removal of features present in the blank and application of an intensity and replicate abundance filter. In positive ionization mode 21,384 features in 5,937 groups remained after filtering. Features were included if they were present in at least 3 out of 4 replicates, therefore the feature number after the application of the filter was higher than in the individual sample. For 706 (positive) and 749 (negative) peaks a match with the suspect list was found. The suspect list contained several isomers, therefore in some cases various molecules were suggested as annotation. Altogether, 1,238 different compounds, partly observed in both ionization modes, were proposed as potential annotations for the feature groups. Identification levels 1-4 were established for 52% (370) and 58% (435) in positive and negative ionization mode, respectively (Table S17 and Table S18). MS2 matches (level  $\geq 3c$ ) were obtained for 187 (positive mode) and 190 (negative mode) feature groups. The annotation of 377 feature groups in both ionization modes with an identification level of at least 3c was successful, consequently showcasing the workflow's ability to not only detect analytes with available reference standard, but also to capture additional compounds potentially present in the samples.

### CONCLUSION

The presented workflow facilitates the rapid and simultaneous exploration of complex environmental exposures and their effect on the human metabolome. Despite issues due to the wide concentration range, the quantification of several endogenous metabolites and exogenous chemicals acquired simultaneously in one short LC-MS/MS run succeeded and correlations between metabolites and chemicals were revealed. Consequently, the effect of certain exposures on the metabolome were directly derived from exposure data in a so far unique way. Combining two columns

and both ionization modes in one single datafile drastically decreased measurement time and simplified data evaluation and storage requirements. For the deciphering of the exposome hundreds to thousands of samples will be needed to be analyzed, therefore the reduced analysis time opens up for so far unseen throughput in exposome-wide association studies for drawing reliable conclusions on the impact of environmental factors on disease development.

### ACKNOWLEDGMENTS

We greatly appreciate the volunteers for donating urine samples and the members of the Warth and Koellensperger labs for critical advice and feedback. We would like to thank the Mass Spectrometry Centre (MSC) of Faculty of Chemistry at the University of Vienna for technical support. This study was financed by the University of Vienna and supported by the ESFRI Research Infrastructure EIRENE.

### CONFLICT OF INTEREST

The authors declare that there are no conflicts of interest.

### AUTHOR INFORMATION

#### Corresponding Author

\*benedikt.warth@univie.ac.at; +43 664 60277 70806

### REFERENCES

- Alderete, T.L., R. Jin, D.I. Walker, D. Valvi, Z. Chen, D.P. Jones, C. Peng, F.D. Gilliland, K. Berhane, D.V. Conti, M.I. Goran, and L. Chatzi. 2019. 'Perfluoroalkyl substances, metabolomic profiling, and alterations in glucose homeostasis among overweight and obese Hispanic children: A proof-of-concept analysis', *Environment International*, 126: 445-53.
- Axelsson, M., J. Sjövall, B.E. Gustafsson, and K.D.R. Setchell. 1982. 'Origin of lignans in mammals and identification of a precursor from plants', *Nature*, 298: 659-60.
- Azzouz, A., A.J. Rascón, and E. Ballesteros. 2016. 'Simultaneous determination of parabens, alkylphenols, phenylphenols, bisphenol A and triclosan in human urine, blood and breast milk by continuous solid-phase extraction and gas chromatography-mass spectrometry', *Journal of Pharmaceutical and Biomedical Analysis*, 119: 16-26.
- Berman, T., R. Goldsmith, T. Göen, J. Spungen, L. Novack, H. Levine, Y. Amitai, T. Shohat, and I. Grotto. 2013. 'Urinary concentrations of environmental contaminants and phytoestrogens in adults in Israel', *Environment International*, 59: 478-84.
- Bloszies, C.S., and O. Fiehn. 2018. 'Using untargeted metabolomics for detecting exposome compounds', *Current Opinion in Toxicology*, 8: 87-92.
- Braun, D., W.A. Abia, B. Šarkanj, M. Sulyok, T. Waldhoer, A.C. Erber, R. Krska, P.C. Turner, D. Marko, C.N. Ezekiel, and B. Warth. 2022. 'Mycotoxin-mixture assessment in mother-infant pairs in Nigeria: From mothers' meal to infants' urine', *Chemosphere*, 287: 132226.
- Braun, D., C.N. Ezekiel, W.A. Abia, L. Wisgrill, G.H. Degen, P.C. Turner, D. Marko, and B. Warth. 2018. 'Monitoring Early Life Mycotoxin Exposures via LC-MS/MS Breast Milk Analysis', *Analytical Chemistry*, 90: 14569-77.
- Chambers, M.C., B. Maclean, R. Burke, D. Amodei, D.L. Ruderman, S. Neumann, L. Gatto, B. Fischer, B. Pratt, J. Egerton, K. Hoff, D. Kessner, N. Tasman, N. Shulman, B. Frewen, T.A. Baker, M.-Y. Brusniak, C. Paulse, D. Creasy, L. Flashner, K. Kani, C. Moulding, S.L. Seymour, L.M. Nuwaysir, B. Lefebvre, F. Kuhlmann, J. Roark, P. Rainer, S. Detlev, T. Hemenway, A. Huhmer, J. Langridge, B. Connolly, T. Chadick, K. Holly, J. Eckels, E.W. Deutsch, R.L. Moritz, J.E. Katz, D.B. Agus, M. MacCoss, D.L. Tabb, and P. Mallick. 2012. 'A cross-platform toolkit for mass spectrometry and proteomics', *Nature Biotechnology*, 30: 918-20.
- Chung, M.K., G.M. Buck Louis, K. Kannan, and C.J. Patel. 2019. 'Exposome-wide association study of semen quality: Systematic discovery of endocrine disrupting chemical biomarkers in fertility require large sample sizes', *Environment International*, 125: 505-14.
- de Oliveira, M.L., B.A. Rocha, V.C.d.O. Souza, and F. Barbosa. 2019. 'Determination of 17 potential endocrine-disrupting chemicals in human saliva by dispersive liquid-liquid microextraction and liquid chromatography-tandem mass spectrometry', *Talanta*, 196: 271-76.
- Ellison, S.L.R., and A. William. 2012. 'EURACHEM/CITAC Guide CG 4-Quantifying Uncertainty in Analytical Measurement', Third Edition.
- Ganna, A., S. Salihovic, J. Sundström, C.D. Broeckling, Å.K. Hedman, P.K.E. Magnusson, N.L. Pedersen, A. Larsson, A. Siegbahn, M. Zilmer, J. Prenni, J. Ärnlöv, L. Lind, T. Fall, and E. Ingelsson. 2014. 'Large-scale Metabolomic Profiling Identifies Novel Biomarkers for Incident Coronary Heart Disease', *PLoS Genetics*, 10: e1004801.

- Garratt, M., K.A. Lagerborg, Y.-M. Tsai, A. Galecki, M. Jain, and R.A. Miller. 2018. 'Male lifespan extension with 17- $\alpha$  estradiol is linked to a sex-specific metabolomic response modulated by gonadal hormones in mice', *Aging Cell*, 17: e12786.
- Helmus, R., T.L. ter Laak, A.P. van Wezel, P. de Voogt, and E.L. Schymanski. 2021. 'patRoom: open source software platform for environmental mass spectrometry based non-target screening', *Journal of Cheminformatics*, 13: 1.
- Hu, X., D.I. Walker, Y. Liang, M.R. Smith, M.L. Orr, B.D. Juran, C. Ma, K. Uppal, M. Koval, G.S. Martin, D.C. Neujahr, C.J. Marsit, Y.-M. Go, K.D. Pennell, G.W. Miller, K.N. Lazaridis, and D.P. Jones. 2021. 'A scalable workflow to characterize the human exposome', *Nature Communications*, 12: 5575.
- Hu, Y., B. Cai, and T. Huan. 2019. 'Enhancing Metabolome Coverage in Data-Dependent LC-MS/MS Analysis through an Integrated Feature Extraction Strategy', *Analytical Chemistry*.
- Iyer, A.P., J. Xue, M. Honda, M. Robinson, T.A. Kumosani, K. Abulnaja, and K. Kannan. 2018. 'Urinary levels of triclosan and triclocarban in several Asian countries, Greece and the USA: Association with oxidative stress', *Environmental Research*, 160: 91-96.
- Jacob, M., A.L. Lopata, M. Dasouki, and A.M. Abdel Rahman. 2019. 'Metabolomics toward personalized medicine', *Mass Spectrometry Reviews*, 38: 221-38.
- Jamnik, T., M. Flasch, D. Braun, Y. Fareed, D. Wasinger, D. Seki, D. Berry, A. Berger, L. Wisgrill, and B. Warth. 2022. 'Next-generation biomonitoring of the early-life chemical exposome in neonatal and infant development', *ChemRxiv*, Cambridge: Cambridge Open Engage.
- Jiang, C., X. Wang, X. Li, J. Inlora, T. Wang, Q. Liu, and M. Snyder. 2018. 'Dynamic Human Environmental Exposome Revealed by Longitudinal Personal Monitoring', *Cell*, 175: 277-91.e31.
- Johnson, C.H., A.D. Patterson, J.R. Idle, and F.J. Gonzalez. 2012. 'Xenobiotic Metabolomics: Major Impact on the Metabolome', *Annual Review of Pharmacology and Toxicology*, 52: 37-56.
- Kang, H., S. Kim, G. Lee, I. Lee, J.P. Lee, J. Lee, H. Park, H.-B. Moon, J. Park, S. Kim, G. Choi, and K. Choi. 2019. 'Urinary metabolites of dibutyl phthalate and benzophenone-3 are potential chemical risk factors of chronic kidney function markers among healthy women', *Environment International*, 124: 354-60.
- Karthikraj, R., S. Lee, and K. Kannan. 2020. 'Biomonitoring of exposure to bisphenols, benzophenones, triclosan, and triclocarban in pet dogs and cats', *Environmental Research*, 180: 108821.
- Koelmel, J.P., N.M. Kroeger, E.L. Gill, C.Z. Ulmer, J.A. Bowden, R.E. Patterson, R.A. Yost, and T.J. Garrett. 2017. 'Expanding lipidome coverage using LC-MS/MS data-dependent acquisition with automated exclusion list generation', *Journal of the American Society for Mass Spectrometry*, 28: 908-17.
- Kolatorova Sosvorova, L., T. Chlupacova, J. Vitku, M. Vlk, J. Heracek, L. Starka, D. Saman, M. Simkova, and R. Hampl. 2017. 'Determination of selected bisphenols, parabens and estrogens in human plasma using LC-MS/MS', *Talanta*, 174: 21-28.
- Liu, X., L. Zhou, X. Shi, and G. Xu. 2019. 'New advances in analytical methods for mass spectrometry-based large-scale metabolomics study', *TRAC Trends in Analytical Chemistry*, 121: 115665.
- MacLean, B., D.M. Tomazela, N. Shulman, M. Chambers, G.L. Finney, B. Frewen, R. Kern, D.L. Tabb, D.C. Liebler, and M.J. MacCoss. 2010. 'Skyline: an open source document editor for creating and analyzing targeted proteomics experiments', *Bioinformatics (Oxford, England)*, 26: 966-68.
- Marin, S., A.J. Ramos, G. Cano-Sancho, and V. Sanchis. 2013. 'Mycotoxins: Occurrence, toxicology, and exposure assessment', *Food and Chemical Toxicology*, 60: 218-37.
- Miller, G.W., and D.P. Jones. 2014. 'The Nature of Nurture: Refining the Definition of the Exposome', *Toxicological Sciences*, 137: 1-2.
- Ougier, E., F. Zeman, J.-P. Antignac, C. Rousselle, R. Lange, M. Kolossa-Gehring, and P. Apel. 2021. 'Human biomonitoring initiative (HBM4EU): Human biomonitoring guidance values (HBM-GVs) derived for bisphenol A', *Environment International*, 154: 106563.
- Pang, Z., J. Chong, G. Zhou, D.A. de Lima Morais, L. Chang, M. Barrette, C. Gauthier, P.-É. Jacques, S. Li, and J. Xia. 2021. 'MetaboAnalyst 5.0: narrowing the gap between raw spectra and functional insights', *Nucleic Acids Research*, 49: W388-W96.
- Paterni, I., C. Granchi, and F. Minutolo. 2017. 'Risks and benefits related to alimentary exposure to xenoestrogens', *Critical Reviews in Food Science and Nutrition*, 57: 3384-404.
- Prasain, J.K., A. Arabshahi, D.R. Moore, 2nd, G.A. Greendale, J.M. Wyss, and S. Barnes. 2010. 'Simultaneous determination of 11 phytoestrogens in human serum using a 2 min liquid chromatography/tandem mass spectrometry method', *Journal of chromatography. B, Analytical technologies in the biomedical and life sciences*, 878: 994-1002.
- Rampl, E., Y.E. Abiead, H. Schoeny, M. Ruz, F. Hildebrand, V. Fitz, and G. Koellensperger. 2021. 'Recurrent Topics in Mass Spectrometry-Based Metabolomics and Lipidomics—Standardization, Coverage, and Throughput', *Analytical Chemistry*, 93: 519-45.
- Rappaport, S.M., D.K. Barupal, D. Wishart, P. Vineis, and A. Scalbert. 2014. 'The blood exposome and its role in discovering causes of disease', *Environmental Health Perspectives*, 122: 769-74.
- Reinke, S.N., H. Gallart-Ayala, C. Gómez, A. Checa, A. Fauland, S. Naz, M.A. Kamleh, R. Djukanović, T.S.C. Hinks, and C.E. Wheelock. 2017. 'Metabolomics analysis identifies different metabolotypes of asthma severity', *European Respiratory Journal*, 49: 1601740.
- Rhoades, S.D., A. Sengupta, and A.M. Weljie. 2017. 'Time is ripe: maturation of metabolomics in chronobiology', *Current Opinion in Biotechnology*, 43: 70-76.
- Šarkanj, B., C.N. Ezekiel, P.C. Turner, W.A. Abia, M. Rychlik, R. Krska, M. Sulyok, and B. Warth. 2018. 'Ultra-sensitive, stable isotope assisted quantification of multiple urinary mycotoxin exposure biomarkers', *Analytica Chimica Acta*, 1019: 84-92.
- Schwaiger, M., H. Schoeny, Y. El Abiead, G. Hermann, E. Rampl, and G. Koellensperger. 2019. 'Merging metabolomics and lipidomics into one analytical run', *Analyst*, 144: 220-29.
- Schymanski, E.L., J. Jeon, R. Gulde, K. Fenner, M. Ruff, H.P. Singer, and J. Hollender. 2014. 'Identifying Small Molecules via High Resolution Mass Spectrometry: Communicating Confidence', *Environmental Science & Technology*, 48: 2097-98.
- Sobus, J.R., J.N. Grossman, A. Chao, R. Singh, A.J. Williams, C.M. Grulke, A.M. Richard, S.R. Newton, A.D. McEachran, and E.M. Ulrich. 2019. 'Using prepared mixtures of ToxCast chemicals to evaluate non-targeted analysis (NTA) method performance', *Analytical and Bioanalytical Chemistry*, 411: 835-51.
- Sofie, C., A. Marta, B. Julie, V. Anne Marie, P. Gitte Alsing, and H. Ulla. 2014. 'Low-dose effects of bisphenol A on early sexual development in male and female rats', *Reproduction*, 147: 477-87.
- Tang, S., T. Li, J. Fang, R. Chen, Y.e. Cha, Y. Wang, M. Zhu, Y. Zhang, Y. Chen, Y. Du, T. Yu, D.C. Thompson, K.J. Godri Pollitt, V. Vasilios, J.S. Ji, H. Kan, J.J. Zhang, and X. Shi. 2021. 'The exposome in practice: an exploratory panel study of biomarkers of air pollutant exposure in Chinese people aged 60–69 years (China BAPE Study)', *Environment International*, 157: 106866.
- Ulrich, E.M., J.R. Sobus, C.M. Grulke, A.M. Richard, S.R. Newton, M.J. Strynar, K. Mansouri, and A.J. Williams. 2019. 'EPA's non-targeted analysis collaborative trial (ENTACT): genesis, design, and initial findings', *Analytical and Bioanalytical Chemistry*, 411: 853-66.
- Vela-Soria, F., I. Jiménez-Díaz, R. Rodríguez-Gómez, A. Zafra-Gómez, O. Ballesteros, A. Navalón, J.L. Vilchez, M.F. Fernández, and N. Olea. 2011. 'Determination of benzophenones in human placental tissue samples by liquid chromatography-tandem mass spectrometry', *Talanta*, 85: 1848-55.
- Vermeulen, R., E.L. Schymanski, A.-L. Barabási, and G.W. Miller. 2020. 'The exposome and health: Where chemistry meets biology', *Science*, 367: 392-96.
- Warth, B., S. Spangler, M. Fang, C.H. Johnson, E.M. Forsberg, A. Granados, R.L. Martin, X. Domingo-Almenara, T. Huan, D. Rinehart, J.R. Montenegro-Burke, B. Hilmers, A. Aisporna, L.T. Hoang, W. Uritboonthai, H.P. Benton, S.D. Richardson, A.J. Williams, and G. Siuzdak. 2017. 'Exposome-Scale Investigations Guided by Global Metabolomics, Pathway Analysis, and Cognitive Computing', *Analytical Chemistry*, 89: 11505-13.
- Wei, F., M. Mortimer, H. Cheng, N. Sang, and L.-H. Guo. 2021. 'Parabens as chemicals of emerging concern in the environment and humans: A review', *Science of the Total Environment*, 778: 146150.
- Wei, T., and V. Simko. 2017. 'R package "corrplot": Visualization of a Correlation Matrix', Available from <https://github.com/taiyun/corrplot>.
- Wenzel, A.G., J.W. Brock, L. Cruze, R.B. Newman, E.R. Unal, B.J. Wolf, S.E. Somerville, and J.R. Kucklick. 2018. 'Prevalence and predictors of phthalate exposure in pregnant women in Charleston, SC', *Chemosphere*, 193: 394-402.
- Wild, C.P. 2005. 'Complementing the Genome with an "Exposome": The Outstanding Challenge of Environmental Exposure Measurement in Molecular Epidemiology', *Cancer Epidemiology Biomarkers & Prevention*, 14: 1847.
- Wolff, M.S., S.L. Teitelbaum, K. McGovern, S.M. Pinney, G.C. Windham, M. Galvez, A. Pajak, M. Rybak, A.M. Calafat, L.H. Kushi, and F.M. Biro. 2015. 'Environmental phenols and pubertal development in girls', *Environment International*, 84: 174-80.
- Xu, Z., J. Liu, X. Wu, B. Huang, and X. Pan. 2017. 'Nonmonotonic responses to low doses of xenoestrogens: A review', *Environmental Research*, 155: 199-207.
- Ye, X., L.-Y. Wong, J. Kramer, X. Zhou, T. Jia, and A.M. Calafat. 2015. 'Urinary Concentrations of Bisphenol A and Three Other Bisphenols in Convenience Samples of U.S. Adults during 2000–2014', *Environmental Science & Technology*, 49: 11834-39.
- Zhang, J., L. Liu, X. Wang, Q. Huang, M. Tian, and H. Shen. 2016. 'Low-Level Environmental Phthalate Exposure Associates with Urine Metabolome Alteration in a Chinese Male Cohort', *Environmental Science & Technology*, 50: 5953-60.
- Zhu, H., S. Chinthakindi, and K. Kannan. 2021. 'A method for the analysis of 121 multi-class environmental chemicals in urine by high-performance liquid chromatography-tandem mass spectrometry', *Journal of Chromatography A*, 1646: 462146.